BOUNDARY-LAYER FLOW OF HEAT AND MASS FOR TIWARI-DAS NANOFLUID MODEL OVER A FLAT PLATE WITH VARIABLE WALL TEMPERATURE

by

Han-Xiang BAO[a], Muhammad BILAL ARAIN[b,c], Sidra SHAHEEN[b], Hasan Izhar KHAN[d], USMAN[e], Mustafa INC[f,g*], and Shao-Wen YAO[a]

[a]School of Mathematics and Information Science, Henan Polytechnic University, Jiaozuo, China
[b]Department of Mathematics and Statistics, International Islamic University, Islamabad, Pakistan
[c]Federal College of Education, Islamabad, Pakistan
[d]Department of Mechanical Engineering, University of engineering and Technology, Lahore, Pakistan
[e]Department of Computer Science, National University of Sciences and Technology, Balochistan Campus, Pakistan
[f]Department of Mathematics, Science Faculty, Firat University, Elazig, Turkey
[g]Department of Medical Research, China Medical University, Taichung, Taiwan

Original scientific paper
https://doi.org/10.2298/TSCI22S1039B

A numerical study of boundary-layer flow past on a moving flat plate in nanofluid with variable wall temperature and viscous dissipation is presented. The PDE containing model for flow phenomena are transformed to ODE with the aid of appropriate similarity transformations. The transformed equations are then solved numerically by using the built-in bvp4c scheme of MATLAB. After the validation of the scheme, numerical solutions are determined for the temperature and nanoparticle concentration profiles along with physical quantities of interest. The effects of involved parameters such as variable temperature index, Prandtl number, Eckert number, Lewis number, plate moving parameter, thermophoresis motion, and Brownian parameters are examined and reported through graphs and tables

Keywords: *boundary-layer flow, moving flat plate, heat and mass transfer, variable wall temperature*

Introduction

Heat and mass transfer phenomena occurs in various engineering applications like paper production, aerodynamics extension of the plastics sheets, glass polymer industry and many others. Main concern of scientists and engineers in all such situations is to achieve a higher heat transfer rate. Enhancement in heat transfer can be obtained through several ways and one of the modern ways is to disperse the nanoparticles in base fluid for such purposes. The idea of such participles comes from the fact that metals have greater thermal conductivity than liquids. The progress in nanotechnology has made it possible to form such metallic parti-

*Corresponding author, e-mail: minc@firat.edu.tr

cles of very small size (nano sized). These small sized particles (1-100 nm) can be mixed in a fluid (called pure fluid) to form a nano-fluid. Maxwell [1] was the first who investigated the flow and heat transfer phenomena with micro sized particles in 1904. Although he noted some heat transfer enhancement, the particle dimensions include radiation absorption. Keblinski *et al.* [2] and Choi and Eastman [3] introduced the word nanofluid for such kinds of fluids. The flow of nanofluid is determined through two groups, single-phase and two-phase models. Single-phase model is discussed further in different ways on the basis of assumption between nanoparticles and base fluid. The most popular single-phase models for nanofluid are Tiwari and Das [4] and Buongiorno [5]. Researchers use these models to investigate the heat and mass transfer phenomena by taking various satiations for example [5-24].

In the present study, the boundary-layer flow of mass concentration in Newtonian fluid with variable conditions at geometry's surface is investigated. The mathematical model is developed by using Tiwari and Das [4] model under viscous dissipation effects. The results of velocity, temperature distribution and mass concentration's flow are calculated under embedding parameters and displayed for discussion.

Mathematical formulation

A steady, incompressible, dimensional boundary-layer flow of nanofluid on a moving flat surface is considered. The velocity, temperature and mass concentration at the wall is taken $u_w(x)$, $T_w(x)$, and $C_w(x)$ and in inviscid region is taken U_∞, T_∞, C_∞, respectively. The geometry of the problem under assumed situation is shown in fig. 1.

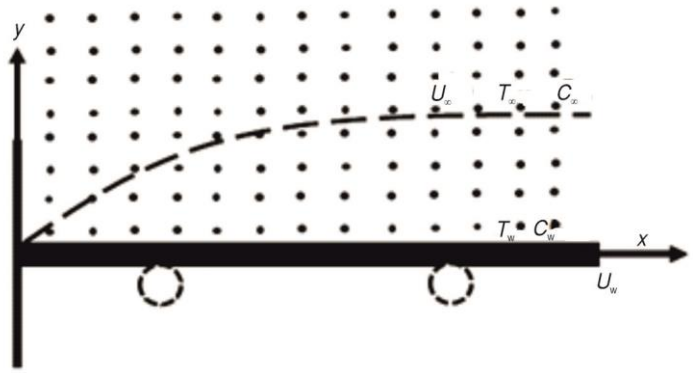

Figure 1. Schematic of flow problem

The Tiwari and Das's governing equation under boundary-layer assumptions are:

$$\frac{\partial u}{\partial x}+\frac{\partial v}{\partial y}=0 \tag{1}$$

$$u\frac{\partial u}{\partial x}+v\frac{\partial v}{\partial y}=\vartheta\frac{\partial^2 u}{\partial y^2} \tag{2}$$

$$u\frac{\partial T}{\partial x}+v\frac{\partial T}{\partial y}=\frac{k}{\rho c_p}\frac{\partial^2 T}{\partial y^2}+\tau\left[D_B\frac{\partial C}{\partial y}\frac{\partial T}{\partial y}+\frac{D_T}{T_\infty}\left(\frac{\partial T}{\partial y}\right)^2\right]+\frac{\mu}{\rho c_p}\left(\frac{\partial^2 y}{\partial y^2}\right)^2 \tag{3}$$

$$u\frac{\partial C}{\partial x}+v\frac{\partial C}{\partial y}=D_B\frac{\partial^2 C}{\partial y^2}+\frac{D_T}{T_\infty}\frac{\partial^2 T}{\partial y^2} \tag{4}$$

along with the boundary conditions:

$$\begin{gathered} u=u_w(x)=\varepsilon x,\ V=0,\ \ T=T_w(x)=nx,\ \ C=C_w(x),\ \text{at}\ \ y=0 \\ u\to U_\infty,\ T\to T_\infty,\ C\to C_\infty,\ \text{at}\ \ y\to\infty \end{gathered} \tag{5}$$

where velocity components are specified with u and v along the x- and y-directions, respectively. The dynamics and kinematic viscosity are specified with μ and ϑ. Further, density, thermal conductivity and specific heat capacity at a constant pressure are specified by ρ, k, and c_p, respectively. Next, D_B, D_T, and τ illustrate the Brownian diffusion coefficient, thermophoresis diffusion coefficient, and the ratio of the effective heat capacity of the nanoparticle materials and the heat capacity of the ordinary fluid respectively.

Now, the governing eqs. (1)-(5) are converted into ODE by using the following similarity transformations as:

$$\eta=\left(\frac{U_\infty}{2\vartheta x}\right)^{\frac{1}{2}}y,\ \ \psi=(2U_\infty\nu x)^{\frac{1}{2}},\ \ \theta(\eta)=\frac{T-T_\infty}{T_w-T_\infty},\ \ \phi(\eta)=\frac{C-C_\infty}{C_w-C_\infty} \tag{6}$$

where θ is the dimensionless temperature of the fluid, ϕ – the rescaled mass concentration, and ψ – the stream function. The velocity components in form of stream function are defined as $u = (\partial\psi/\partial y)$ and $v = (\partial\psi/\partial x)$ which identically satisfied the continuity eq. (1). The velocity components u and v can be derived by using eq. (6) as:

$$u=U_\infty f'(\eta),\ \ v=-\left(\frac{U_\infty\vartheta}{2x}\right)^{\frac{1}{2}}f(\eta)+\frac{U_\infty y}{2x}f'(\eta) \tag{7}$$

In view of eqs. (6) and (7), the eqs. (2)-(4) become:

$$f'''+ff''=0 \tag{8}$$

$$\frac{1}{\mathrm{Pr}}\theta''+f\ \theta'-2n\theta f'+N_b\theta'\phi'+N_t\theta'^2+\mathrm{Ec}\,f''^2=0 \tag{9}$$

$$\phi''+\frac{N_t}{N_b}\theta''+\mathrm{Le}\,f\phi'=0 \tag{10}$$

where

$$\mathrm{Pr}=\frac{\vartheta\rho c_p}{k},\ N_b=\frac{\tau D_B(C_w-C_\infty)}{\vartheta},\ N_t=\frac{\tau D_T\lfloor D_B(T_w-T_\infty)\rfloor}{T_\infty\vartheta},\ \mathrm{Ec}=\frac{U_\infty^2}{C_p(T_w-T_\infty)},\ \text{and}\ \mathrm{Le}=\frac{\vartheta}{D_B}$$

represent the Prandtl number, Brownian motion parameter, thermophoresis parameter, Eckert number, and Lewis number, respectively. The boundary conditions (5) take the form:

$$\begin{gathered} f(0)=0,\ f'(0)=\varepsilon,\ \ \theta(0)=1,\ \ \phi(0)=1 \\ f'(\eta)\to1,\ \theta(\eta)\to0,\ \phi(\eta)\to0\ \text{as}\ \eta\to\infty \end{gathered} \tag{11}$$

Note that $\varepsilon > 0$ corresponds to the downstream movement of the surface from the origin. The physical quantities of the interest C_f, the local Nusselt number Nu_x, and Sherwood number Sh_x which are described by:

$$C_f = \frac{t_w}{\rho u_e^2},\ \mathrm{Nu}_x = \frac{x q_w}{k(T_w - T_\infty)},\ \mathrm{Sh}_x = \frac{x j_w}{D_B(C_w - C_\infty)} \tag{12}$$

where the quantities t_w, q_w, and j_w are the surface shear stress, surface heat flux, and surface mass flux, respectively. These quantities are defined as:

$$t_w = \mu\left(\frac{\partial u}{\partial y}\right)_{y=0},\ q_w = -k\left(\frac{\partial T}{\partial y}\right)_{y=0},\ j_w = -D_B\left(\frac{\partial C}{\partial y}\right)_{y=0} \tag{13}$$

Using the similarity transformations given in eq. (6), eq. (12) become:

$$C_f = (2\mathrm{Re}_x)^{-\frac{1}{2}} f''(0),\ \mathrm{Nu}_x = -\left(\frac{\mathrm{Re}_x}{2}\right)^{-\frac{1}{2}} \theta'(0),\ \mathrm{Sh}_x = -\left(\frac{\mathrm{Re}_x}{2}\right)^{-\frac{1}{2}} \phi'(0) \tag{14}$$

where $\mathrm{Re}_x = (U_\infty x/\vartheta)$ is the local Reynolds number.

Numerical solution

In this section, the governing eqs. (8)-(11) subject to eq. (12) are solved by numerically with the aid of bvp4c scheme of MATLAB. The validity and accuracy of the method is confirmed by reproducing the results of Nusselt number, Sherwood number, and skin friction coefficient in tab. 1. Table 1 shows the comparison of the values reported in [25] and the values obtained in the present results are in good agreement with the results of [25].

Table 1. Comparison of values of Nusselt number, Sherwood number, and skin coefficient number with [25] for various values of ε by fixing Pr = 7, $N_b = N_t$ = Ec = 0.1, and Le = 10

	Nu_x		Sh_x		C_f	
ε	[25]	Present	[25]	Present	[25]	Present
0	0.3747	0.3746	1.1672	1.1670	0.4696	0.4696
0.1	0.4705	0.4704	1.3379	1.3367	0.4625	0.4625
0.5	0.7875	0.7874	1.8657	1.8655	0.3288	0.3287
1	1.0717	1.0717	2.3805	2.3805	0	0
2	1.2994	1.2990	3.3099	3.3090	−1.0191	−1.0191

Results and discussion

The effects of the involved parameters such as variables temperature index n, Prandtl number, the plate velocity parameter ε, thermophoresis parameter N_t, Brownian motion parameter N_b, Eckert number, and Lewis number on temperature θ and mass concentration ϕ are reported through graphs and tables. Figures 2-5 show the temperature profiles for the involved parameters n, Prandtl number, ε, N_t, and N_b. Figure 2 shows the effect of variables temperature parameter n on the temperature profile. It shows that the temperature profile decreases by increasing n. The effects of Prandtl number on the thermal boundary-layer thickness are shown in fig. 3. The temperature profile decreases as Prandtl number increases. Figure 4 shows the effects of the plate velocity parameter ε on the temperature profile. By increasing ε, the temperature profile decreases. Practically, the increment in ε increases ratio velocity differences between the plate and the fluid which enhance the fluid to move away from the surface region rapidly. Figure 5 shows the effects of the N_b and N_t on the temperature profile. The temperature profile increases as N_b and N_t increase. Figures 6 and 7 illustrate the behaviours of mass concentration for various values of involved parameters. Figure 6 shows

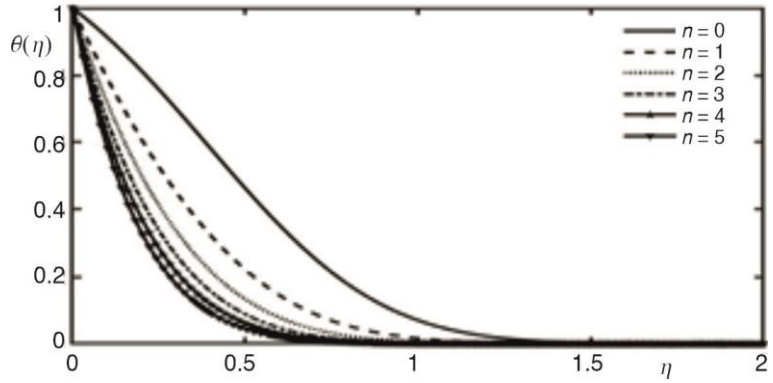

Figure 2. Effects of variable temperature parameter *n* on the thermal boundary-layer thickness $\theta(\eta)$ by fixingPr = 7, ε = 0.5, $N_b = N_t$ = Ec = 0.1, and Le = 10

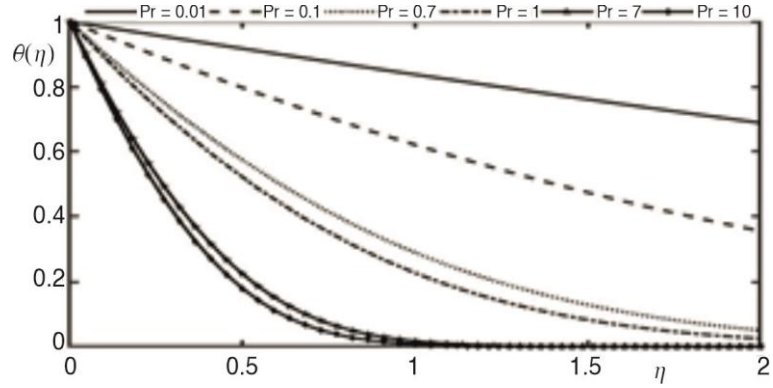

Figure 3. Effects of Prandtl number on the thermal boundary-layer thickness $\theta(\eta)$ by fixing *n* = 1, ε = 0.5, $N_b = N_t$ = Ec = 0.1, and Le = 10

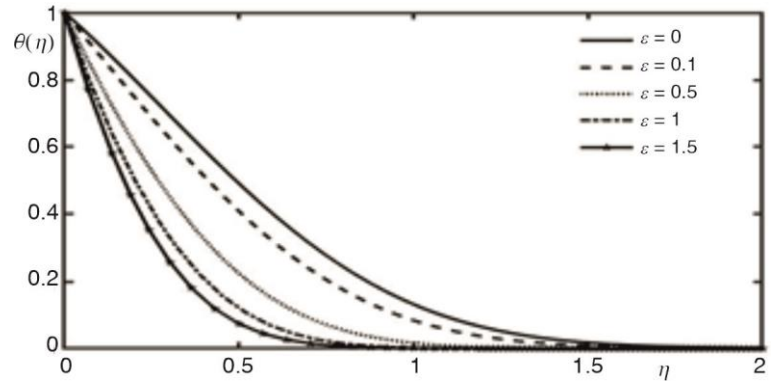

Figure 4. Effects of plate velocity parameter ε on the thermal boundary-layer thickness θ(η) by fixing *n* = 1, Pr= 7, $N_b = N_t$ = Ec = 0.1, and Le = 10

the effects of N_b and ε on the mass concentration flow. As N_b increases, the mass concentration flow decreases. The parameter ε also affects the flow of mass concentration in similar way. Figure 7 shows the effects of the N_t and Lewis number on the flow of mass concentra-

tion. Both parameters effect the flow of mass concentration oppositely. The mass concentration flow increases as N_t increases and decreases by increasing Lewis number. The effect of n, Prandtl number, ε, Lewis number, and Eckert number parameters on the local Nusselt number are shown in tabs. 2-4. The values of $(\mathrm{Re}_x/2)^{1/2}\mathrm{Nu}_x$ is increased by n parameter but decreased by Eckert number as seen in tab. 2. In tab. 3, it is found that $(\mathrm{Re}_x/2)^{1/2}\mathrm{Nu}_x$ increases and decreases by increasing of Prandtl and Lewis numbers, respectively. The behaviour of $(\mathrm{Re}_x/2)^{1/2}\mathrm{Nu}_x$ is increased with increasing of ε as displayed in tab. 4.

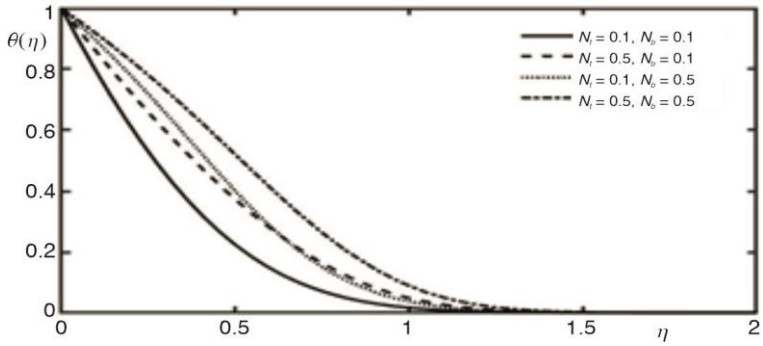

Figure 5. Effects of Nb and Nt on the thermal boundary-layer thickness θ(η) by fixing n = 1, Pr = 7, ε = 0.5, Ec = 0.1, and Le = 10

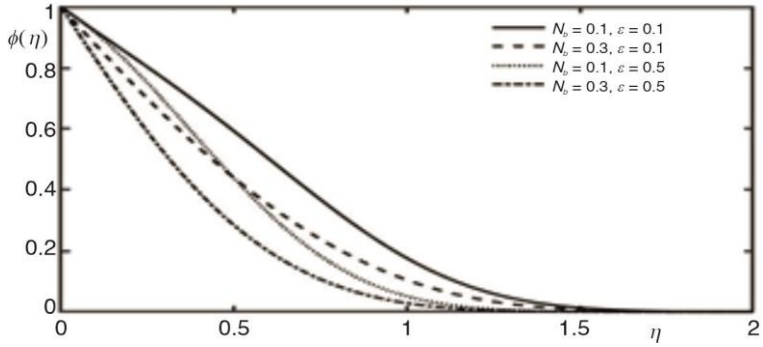

Figure 6. Effects of N_b and ε on the nanoparticle volume fraction $\phi(\eta)$ by fixing n = 1, Pr = 7, N_t = Ec = 0.1, and Le = 10

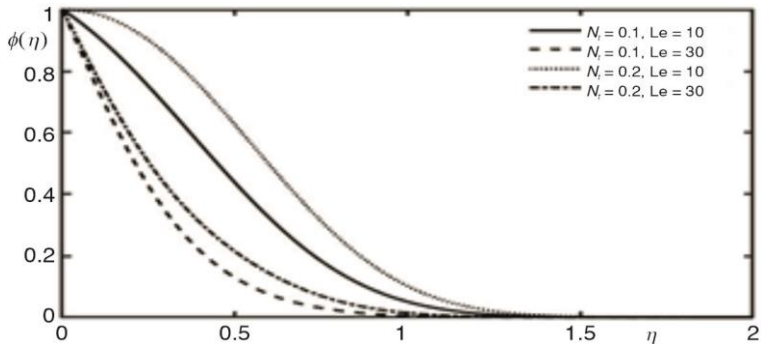

Figure 7. Effects of N_t and Lewis numberon the nanoparticle volume fraction $\phi(\eta)$ by fixing n = 1, Pr = 7, ε = 0.5, and N_b = Ec = 0.1

Table 2. Values of Nusselt number for various values of *n* by fixing Pr = 7, $\varepsilon = 0.5$, $N_b = N_t = 0.1$, and Le = 10

	Ec = 0	Ec = 0.1	Ec = 0.3
n	$\left(\frac{\mathrm{Re}_x}{2}\right)^{1/2}\mathrm{Nu}_x$	$\left(\frac{\mathrm{Re}_x}{2}\right)^{1/2}\mathrm{Nu}_x$	$\left(\frac{\mathrm{Re}_x}{2}\right)^{1/2}\mathrm{Nu}_x$
0	0.8148	0.7874	0.7324
1	2.2199	2.2032	2.1697
2	3.1626	3.1492	3.1224

Table 2. Values of Nusselt number for various values of Prandtl number by fixing $n = 1$, $\varepsilon = 0.5$, $N_b = N_t = 0.1$, and Ec = 10

	Le = 10	Le = 20	Le = 30
Pr	$\left(\frac{\mathrm{Re}_x}{2}\right)^{1/2}\mathrm{Nu}_x$	$\left(\frac{\mathrm{Re}_x}{2}\right)^{1/2}\mathrm{Nu}_x$	$\left(\frac{\mathrm{Re}_x}{2}\right)^{1/2}\mathrm{Nu}_x$
9	2.3452	2.1326	2.0115
30	2.8666	2.3831	2.1233
50	2.9821	2.4112	2.1168

Table 4. Values of Nusselt number for various values of ε by fixing $n = 1$, Pr = 7, $N_b = N_t = 0.1$, and Le = 10

	Ec = 0	Ec = 0.1	Ec = 0.3
ε	$\left(\frac{\mathrm{Re}_x}{2}\right)^{1/2}\mathrm{Nu}_x$	$\left(\frac{\mathrm{Re}_x}{2}\right)^{1/2}\mathrm{Nu}_x$	$\left(\frac{\mathrm{Re}_x}{2}\right)^{1/2}\mathrm{Nu}_x$
0	0.9553	0.9003	0.7897
1.0	3.0340	3.0340	3.0340
2.0	4.2271	4.1327	3.9431

Conclusion

In current study, the behavior of heat and mass distribution is discussed by Tiwari and Das model under variable boundary conditions when mass concentration is exited in Newtonian fluid. The physical model is solved by numerical method and results are displayed for distribution of temperature and mass. From the result, it is found that the distribution of temperature is increased with the effects of N_b and N_t and decreased by *n*, Prandtl number, and ε. The flow of mass concentration is enhanced by N_t and Prandtl number, but declined by Lewis number, N_b, and ε.

Funding

National Natural Science Foundation of China (No. 71601072), the Fundamental Research Funds for the Universities of Henan Province (No. NSFRF210314) and Innovative Research Team of Henan Polytechnic University (No. T2022-7).

References

[1] Maxwell, J. C., *Theory of Hea*t, Oxford University Press, London, UK, 1904
[2] Keblinski, P., *et al*., Mechanisms of Heat Flow in Suspensions of Nano-Sized Particles (Nanofluids), *Int. J. Heat Mass Transf., 45* (2002), 4, pp. 855-863
[3] Choi, S. U., Eastman, J. A., Enhancing Thermal Conductivity of Fluids with Nanoparticles (No. ANL/MSD/CP-84938; CONF-951135-29), Argonne National Lab., Argone, Ill, USA, 1995
[4] Tiwari, R. K., Das, M. K., Heat Transfer Augmentation in a Two-Sided Lid-Driven Differentially Heated Square Cavity Utilizing Nanofluids, *International Journal of heat and Mass transfer, 50* (2007), 9-10, pp. 2002-2018
[5] Buongiorno, J., Convective transport in nanofluids, *Jou. of Heat Transfer, 128* (2006), 3, pp. 240-250
[6] Machireddy, G. R., *et al*., Effects of Magnetic Field and Ohmic Heating on Viscous Flow of a Nanofluid Towards a Nonlinear Permeable Stretching Sheet, *Journal of Nanofluids, 5* (2016), 3, pp. 459-470
[7] Sakiadis, B. C., Boundary-Layer Behavior on Continuous Solid Surfaces: I. Boundary-Layer Equations for Two Dimensional and Axisymmetric Flow, *American Institute of Chemical Engineers (AIChE) Journal, 7* (1961), 1, pp. 26-28
[8] Crane, L. J., Flow Past a Stretching Plate, *Zeitschrift für angewandte Mathematik und Physik ZAMP, 21* (1970), 4, pp. 645-647
[9] Rehman, S. U., *et al*., Impact of Cattaneo-Christov Heat Flux Model on the Flow of Maxwell Ferromagnetic Liquid Along a Cold Flat Plate Embedded with Two Equal Magnetic Dipoles, *J. Magn, 22* (2017), 3, pp. 472-477
[10] Kakac, S., Pramuanjaroenkij, A., Review of convective heat transfer enhancement with nanofluids, *Int. J. Heat Mass Transf., 52* (2009), 13-14, pp. 3187-3196
[11] Gnaneswara, M. R., Influence of Magnetohydrodynamic and Thermal Radiation Boundary Layer Flow of a Nanofluid Past a Stretching Sheet, J. Sci. Res., 6 (2014), 2, pp. 257-272
[12] Hassan, M., Impact of Iron Oxide Particles Concentration Under a Highly Oscillating Magnetic Field on Ferrofluid Flow, *The European Physical Journal Plus, 133* (2018), 6, pp. 1-14
[13] Ishak, A., *et al*., Radiation Effects on the Thermal Boundary-Layer Flow over a Moving Plate with Convective Boundary Condition, *Meccanica; 46* (2011), 4, pp. 795-801
[14] Hassan, M., *et al*., The Effects of Zero and High Shear Rates Viscosities on the Transportation of Heat and Mass in Boundary-Layer Regions: A Non-Newtonian Fluid with Carreau Model, *Journal of Molecular Liquids, 317* (2020), 113991
[15] Fetecau, C., *et al*., Analytical Solutions for Two Mixed Initial-Boundary Value Problems Corresponding to Unsteady Motions of Maxwell Fluids through a Porous Plate Channel, *Mathematical Problems in Engineering, 2021* (2021), ID5539007
[16] Hassan, M., *et al*., Effects of Cu–Ag Hybrid Nanoparticles on the Momentum and Thermal Boundary-Layer Flow Over the Wedge, Proceedings of the Institution of Mechanical Engineers, *Part E: Journal of Process Mechanical Engineering, 233* (2019), 5, pp. 1128-1136
[17] Vajravelu, K., Hadjinicolaou, A., Heat Transfer in a Viscous Fluid Over a Stretching Sheet with Viscous Dissipation and Internal Heat Generation, *International Communications in Heat and Mass Transfer, 20* (1993), 3, pp. 417-430
[18] Hassan, M., *et al*., Assessment of Boundary-Layer for Flow of Non-Newtonian Material Induced by a Moving Belt with Power Law Viscosity and Thermal Conductivity Models, *Numerical Methods for Partial Differential Equations*, On-line first, https://doi.org/10.1002/num.22743, 2021
[19] Hassan, M., *et al*., Transport Pattern of Non-Newtonian Mass and Thermal Energy Under Two Diverse Flow Conditions by Using Modified Models for Thermodynamics Properties, *Case Studies in Thermal Engineering, 29* (2022), 101714
[20] Yirga, Y., Shankar, B., Effects of Thermal Radiation and Viscous Dissipation on Magnetohydrodynamic Stagnation Point Flow and Heat Transfer of Nanofluid Towards a Stretching Sheet, *Journal of Nanofluids; 2* (2013), 4, pp. 283-291
[21] Menni, Y., *et al.*, Heat and Mass Transfer of Oils in Baffled and Finned Ducts, *Thermal Science, 24* (2021), Suppl. 1, pp. S267-276
[22] Asadullah, M., *et al*, Mathematical Fractional Modeling of Transpot Phenomena of Viscous Fluid-Flow Between Two Plates, *Thermal Science, 25* (2021), Special Issue 2, pp. S417-S421
[23] Arshed, S., *et al*, Soliton Solutions for Non-Linear Kudryashov's Equation via Three Integrating Schemes, *Thermal Science, 25* (2021), Special Issue 2, pp. S157-S163

[24] Ulutas, E., *et al*., Exact Solutions Of Stochastic Kdv Equation With Conformable Derivatives In White Noise Environment, *Thermal Science, 25* (2021), Special Issue 2, pp. S143-S149
[25] Anuar, M. M., *et al*., Boundary-Layer Flow over a Moving Plate in a Nanofluid with Viscous Dissipation, *Proceedings*, 3rd International Conference on Computer Engineering and Mathematical Sciences (ICCEMS 2014), Langkawi, Malaysia

Paper submitted: August 15, 2022
Paper revised: September 25, 2022
Paper accepted: October 13, 2022